

Real Structure and Physical Properties of Chromites as an Indicator of Their Genesis

S. A. Svetov¹, A. D. Fofanov², V. F. Smol'kin³, E. V. Moshkina³,
E. A. Repnikova², and V. I. Kevlich¹

Presented by Academician N.P. Yashkin June 25, 2003

Received July 9, 2003

Spinel (Mg, Fe^{2+})(Cr, Al, Fe^{3+})₂O₄ are the most informative minerals for reconstruction of *PT* crystallization parameters and differentiation conditions of ultramafic melts [1]. It is known that the real structure and physical properties of spinels are governed by their formation conditions (chemical composition of the melt, temperature and pressure of crystallization, and others) [2, 3].

The cation composition of spinels correlates with chemical composition of the host rocks (picrites, komatiites) and more often corresponds to magnoaluminochromites. Spinel shows an increase in Fe content and changes from chromites to ferrochromites and titanomagnetites during magmatic differentiation.

The good preservation of spinels during metamorphism (preservation of crystal relicts up to amphibolite facies with replacement of rims by the later magnetite and formation of zones of intermediate composition [4, 5]) serves as an additional argument for their application as paleothermometers and barometers.

Therefore, the search for and selection of the most efficient structural and physical characteristics of Cr-spinels for genetic reconstruction are of great importance. Our investigation is aimed at revealing the reliably fixed differences in X-ray powder diffraction patterns of chromites from different deposits and correct interpretation of the observed effects on the basis of real structures formed during crystallization.

The term "real chromite structure" implies information on point defects of crystalline lattice, packing defects, sizes of coherent scattering domains, and

microdistortions, as well as composition and distribution of cations in octahedral and tetrahedral sites of the anion sublattice.

The study objects were spinels from the Fennoscandian chromite deposits and occurrences, confined to the Early Proterozoic layered intrusion (2.50–2.44 Ga) of the Kola Peninsula (Moncha Pluton, Pados), Karelia (Burakov Massif), and Finland (Kemi). For comparison, we used chromites from the ophiolite-type Kempirsai deposit.

Samples (Table 1) were studied with electron and optical microscopy. The morphology of grains was analyzed on an REM-20 scanning electron microscope at the Geological Institute of the Karelian Scientific Center. Element contents were measured on a Cameca MS-46 microprobe at the Geological Institute of the Kola Scientific Center. The chromite content in ores from different deposits ranges between 40 and 98 vol %. Chromite occurs in densely disseminated ores as homogeneous euhedral grains and aggregates with silicate cement (pyroxenes and their alteration products). Some grains occur as poikilitic inclusions in olivine. In massive ores, chromite forms a mosaic solid mass, which occasionally contains altered olivine.

For extraction of monomineral fractions, we developed a scheme taking into consideration the mineral composition, grain size, main technological properties of chromites, and earlier applied techniques [6, 7]. Ore samples were crushed to –0.16 mm with the subsequent removal of fraction –0.5 mm. Concentration in heavy liquids (density 3.0 and 4.2 g/cm³) made it possible to separate main rock-forming and accessory minerals (light fraction) from chromite (heavy fraction). Then, the heavy fraction was subjected to ultrasonic treatment for cleaning the surface. The XRD patterns of the obtained monofractions showed that the samples are monophase chromites. No reflections of other minerals were observed.

In most cases, chromite grains have a homogeneous structure with occasional zoning (Pados) developed during magmatic differentiation as a response to the decrease of crystallization temperature and increase in

¹ Institute of Geology, Karelian Scientific Center,
Russian Academy of Sciences,
Pushkinskaya ul. 11, Petrozavodsk, Karelia, 185610 Russia;
e-mail: ssvetov@krc.karelia.ru

² Petrozavodsk State University,
pr. Lenina 33, 185640 Russia

³ Geological Institute, Kola Scientific Center,
Russian Academy of Sciences,
ul. Fersmana 14, Apatity, Murmansk oblast, 184200 Russia

Fe content relative to Cr. The subsequent postmagmatic serpentinization promoted oxidation of some Fe into the three-valent state and replacement of chromite by magnetite. Zoned crystals show significant chemical variations. The core equilibrium with primary high-Mg melt is characterized by high contents of the following components (wt %): Cr₂O₃ (up to 53), MgO (up to 8), Al₂O₃ (up to 12), and ZnO (up to 1.8). Rims are enriched in FeO (up to 65), MnO (up to 1.6), NiO (up to 0.45), and TiO₂ (up to 0.59) (Table 2). Measurements of physicochemical properties indicated a significant variability of density, magnetic susceptibility, and electric resistance. Density positively correlates with chromite content (vol %) in the ore, while magnetic susceptibility correlates with the chemical composition of spinels (in particular, magnetite in rims of zoned crystals) [8].

The real structure of obtained chromite monofractions was estimated by X-ray analysis.

The determination of lattice spacings of chromites (based on the position of diffraction bands within precision range) made it possible to discover that lattices of some samples are deformed along the solid cubic diagonal, thus changing the distance between closely packed anion sheets with respect to that of an ideal cubic lattice [8]. This fact indicates the difference in cation distribution in spinel sites of the closest oxygen packing depending on crystallization conditions. The unit cell spacing ranges within 8.299–8.318 Å for chromite samples and is equal to 8.390 Å, which is close to that of magnetite, for magnetite-bearing samples [9, 10].

In order to determine the efficiency of standard full-profile method (Rietveld method) for obtaining information on the real structure of natural Cr-spinels, we refined the structural parameters of four samples which differ most strongly in magnetic and electric properties [8]. The calculations were performed assuming that the studied samples have an *Fd3m* space group and are ascribed to the normal spinels. The lattice spacings determined by the Rietveld method are consistent with those found in independent experiments on precision determination of lattice spacings [8]. The oxygen parameters exhibit narrow variations and, hence, are insufficiently informative for the estimation of cation distribution in genetically different Cr-spinels. The site occupation coefficients, which mainly characterize the presence of vacancies in the corresponding position of unit cell, show an insignificant variation between samples. The mean-square displacement of cations and anions from equilibrium are within reported variations for synthetic spinels [8]. No data are available on the study of natural spinels by the Rietveld method. The mean-square displacements are related to both thermal vibrations and statistic displacements caused by lattice defects.

These results indicate that the refinement of real structure by the Rietveld method can be improved by

Table 1. Mineralogical composition of studied chromite ores

Sample no.	Mineralogical composition (vol %)
F-15/1	Chromite (74), pink chlorite (25), tremolite (1), actinolite, olivine, diopside, and epidote (s.g.)
Kemp-4	Chromite (98–99), chlorite, biotite, olivine, orthopyroxene, pink garnet, actinolite-tremolite, uvarovite, plagioclase, and quartz (s.g.)
C-1585/132.6	Chromite (95), tremolite + pink chlorite (5), biotite, and olivine orthopyroxene (s.g.)
C-1508/50.8	Chromite (50), antigorite (47), tremolite (3), chlorite, biotite, olivine, orthopyroxene, diopside, and calcite (s.g.)
Bur-1	Chromite (85), clinopyroxene + orthopyroxene + serpentine + olivine (15), garnet, biotite, and calcite (s.g.)
M-36	Chromite (40), orthopyroxene + diopside + olivine + actinolite + serpentine (60), leucogenized titanite, feldspar, and talc (s.g.)
K-132/1	Chromite (78), pink chlorite (22)
P-103.1/15	Chromite (93), chlorite + scapolite + muscovite + orthopyroxene (7), hornblende and tourmaline (s.g.)

Note: (F 15/1) Densely disseminated ore, quarry at the Kemi deposit, Finland; (Kemp-4) massive ore, quarry at the Kempirsai deposit, Kazakhstan; (C-1585/132.6 and C-1508/50.8) rich banded ore, central part of the Sopcha deposit, Moncha Pluton, Kola Peninsula, borehole core; (Bur-1) densely disseminated ore, main chromite horizon of the Burakov Massif, eastern Karelia, bedrock; (M-36) nodular chromitite from the alternation zone of bronzitites and harzburgites, Kumuzh'ya Mount, Moncha Pluton, Kola Peninsula, block; (K-132/1) vein metamorphosed ore, ore occurrence in the Pados Massif, exploration trench, Kola Peninsula; (P-103.1/15) massive stratified ore, ore occurrence in the Pados Massif, Kola Peninsula, bedrock; (s.g.) single grains.

decrease of lattice symmetry. It should be noted that the Rietveld method is based on the kinematic approximation of the X-ray scattering theory, which applies the totality of randomly disoriented crystallites with coherent scattering domains significantly lower than extinction length as a model polycrystalline object. The refinement procedure is based on formulas that do not allow one to obtain more detailed information on the object. The curves in the Rietveld method are approximated by functions whose parameters are not directly related with the real physical state of constituent crystallites.

The X-ray powder diffraction pattern [3] provides quantitative information not only on sizes of coherent scattering domains (CSD) and microdistortions but also on packing defects, whose presence and type are directly related to the formation conditions of crystals.

The approximation of integral width of diffraction bands in XRD patterns showed that almost all studied samples reveal the same (within measurement error) slope of the function $\beta \cos \vartheta = f(\sin \vartheta)$ in [100] and [311] directions, as well as [111] and [211] directions, where

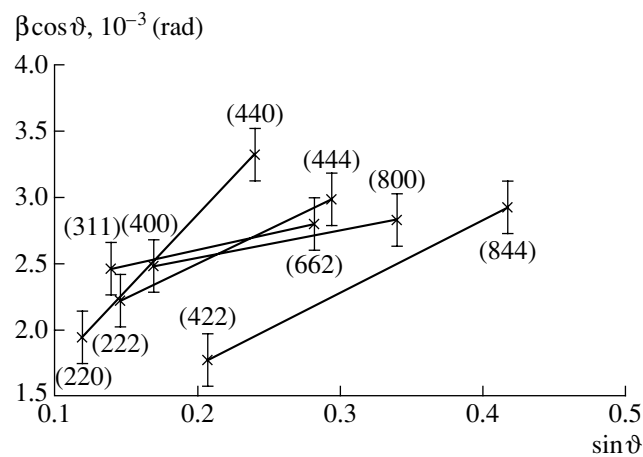
Table 2. Chemical composition of ore chromites, wt %

Sample no.	Zone	Cr ₂ O ₃	Al ₂ O ₃	MgO	FeO	MnO	ZnO	NiO	TiO ₂	Total	FeO*	Fe ₂ O ₃ *
F-15/1		48.61	15.12	10.98	20.35	0.26	0.02	0.04	0.47	96.11	16.51	3.84
Kemp-4		60.09	7.89	13.24	13.19	0.12		0.13	0.1	94.76	11.26	1.93
C-1585/132.6		58.15	10.43	13.99	14.52	0.49		0.17	0.11	97.85	11.13	3.39
C-1508/50.8		56.06	12.37	15.65	13.89	0.33		0.17	0.22	98.68	9.44	4.45
Bur-1a		54.77	8.36	10.48	22.05	0.64	0.2	0.24	1.22	97.95	16.84	5.21
Bur-1b		55.14	7.96	10.51	22.23	0.59	0.16	0.24	1.18	98.01	16.80	5.43
M-36		51.87	7.36	12.79	25.88	0.02	0.09	0.12	0.57	98.72	13.77	12.11
K-132/1a	C	35.31	11.41	6.37	45.37	0.89		0.07	0.16	99.58	23.59	21.78
K-132/1a	E	26.33	0.36	3.1	64.58	0.97		0.32	0.14	95.8	25.61	38.96
K-132/1b	C	31.94	10.93	6.35	47.17	0.94		0.05	0.18	97.56	22.92	24.24
K-132/1b	E	26.02	0.28	2.57	64.08	0.86		0.45	0.3	94.57	26.13	37.95
P-103.1/15a	C	50.54	11.85	7.71	25.14	1.2	1.3	0.03	0.61	98.38	19.85	5.29
P-103.1/15a	E	40.61	0.25	3.17	53.17	1.33	0.49	0.4	0.51	99.92	26.04	27.13
P-103.1/15b	C	50.81	10.06	6.81	27.25	0.66	1.82	0.63	0.24	98.28	20.09	7.16
P-103.1/15b	E	22.86	0.24	3.14	64.59	0.42	0.5	0.42	0.59	92.74	24.97	39.61
P-103.1/15c	C	52.66	10.31	6.53	25.87	0.64	1.82	0.05	0.24	98.14	21.05	4.82
P-103.1/15c	E	42.24	0.43	3.85	48.62	1.61	0.53	0.27	0.48	98.02	24.15	24.47

Note: (F-15/1) Chromite in densely disseminated fine-grained ore, chloritized serpentinite cement (average from seven analyses); (Kemp-4) chromite in massive coarse-grained ore; (C-1585/132.6, C-1508/50.8) chromite from massive ore interbeds in banded ores; (Bur 1) chromite in densely disseminated fine-grained ore with peridotite cement: (a, b) different parts of the sample; (M-36) chromite-rich nodule in olivine bronzitites with sideronite structure; (K-132/1) chromite with an intricate zoning in the massive, vein metamorphosed ore and fine-grained structure: (a, b) different parts of the grain; (P-103.1/15) zoned chromite in an 8-cm-thick massive ore bed: (a) lower part, (b) central part, (c) upper part; (FeO*, Fe₂O₃*) calculated for stoichiometric composition; (F-15/1) contains 0.14 wt % CoO.

(C) Grain center, (E) grain edge. Samples were provided by V.F. Smol'kin and analyzed by Ya.A. Pakhomovskii and S.A. Ryazhenova (Geological Institute, Kola Scientific Center).

β is the physical widening of diffraction peaks and ϑ is their scattering angle. The figure shows dependence for Sample K-132/1 (center) indicating nearly a similar contribution of microdistortions ($\Delta a/a \sim 0.001\text{--}0.003$) to physical widening. The CSD size in different directions varies within 300–600 Å. The discovered regularities suggest a contribution of diffraction bands of growth dislocations and packing defects, whose contents are different in the core and rim of zoned chromites, to the integral width.



Plot $\beta \cos \vartheta = f(\sin \vartheta)$ for Sample K-132/1 (center).

The X-ray diffraction patterns of fine chromite monocrystals ($\sim 0.2\text{--}1$ mm), which were extracted from minerals, make it possible to determine the low-angle boundaries existing within a mosaic crystal. In particular, the epigram of euhedral chromite from the Burakov Massif demonstrates split reflections, which indicates a mosaic structure of crystals. The splitting of spots in the epigram suggests that mosaic blocks are rotated relative to each other at a small angle due to the sagging or twisting of crystals. The latter may be caused by tensions during crystal growth [11]. The average disorientation angle is $\sim 44''$ ($2.2 \cdot 10^{-4}$ rad). The absence of such diffuse reflections in the epigram of xenomorphic monocrystals indicates that they are less distorted and more perfect.

Thus, we discovered the reliably registered differences in X-ray powder diffraction patterns between genetically different chromites.

The correct interpretation of observed effects using models of a real structure makes it possible to estimate the crystallization conditions of chromites.

However, the establishment of correlation of the real structure of Cr-spinels, as well as composition and distribution of cations in octahedral and tetrahedral sites of anionic sublattice, with thermodynamic crystallization

conditions requires the computer simulation of specific parameters of the real microcrystalline structure of studied objects and degree of its deviation from the ideal spinel lattice. Atomic clusters of a certain composition at temperatures and pressures corresponding to the inferred crystallization conditions of these minerals should also be calculated. The comparison of structural characteristics of the newly formed clusters with the experimentally determined unit cell parameters of the real Cr-spinel structure makes it possible to estimate the energetic preference of structural states observed in studied minerals.

ACKNOWLEDGMENTS

We are grateful to E.A. Nikitina (Petrozavodsk State University) for help in performing X-ray investigations.

This study was supported by the Russian Foundation for Basic Research (project nos. 01-05-64228, 02-05-06207).

REFERENCES

1. Matsyuk, S.S., Platonov, A.N., Pol'shin, E.V., *et al.*, *Shpinelidy mantiinykh porod* (Spinels from Mantle Rocks), Kiev: Naukova Dumka, 1989.
2. Varshavskii, M.T., Pashchenko, V.P., Men', A.N., *et al.*, *Defektnost' struktury i fiziko-khimicheskie svoystva fer-roshpinelei* (Defects of Structure and Physicochemical Properties of Ferros spinels), Moscow: Nauka, 1988.
3. Fadeeva, V.I., *Real'naya struktura oksidnykh faz tipa shpineli i korunda* (Real Structure of the Oxide Phase of Spinel and Corundum Types), *Doctoral (Phys.-Math.) Dissertation*, Moscow: Mosk. Gos. Univ., 1983.
4. Irvine, T.N., *Can. J. Earth Sci.*, 1965, vol. 2, pp. 648–672.
5. Irvine, T.N., *Can. J. Earth Sci.*, 1967, vol. 4, pp. 71–103.
6. Chanturiya, V.A., *Vestn. OGGGGN Ross. Akad. Nauk*, 1998, no. 4(6), pp. 39–62.
7. Kurochkin, M.G., *Obogashchenie khromitovykh rud* (Dressing of Chromite Ores), Novosibirsk: Nauka, 1998.
8. Fofanov, A.D., Svetov, S.A., Kevlich, V.I., *et al.*, *Elektron. Zh. "Issledovano v Rossii,"* 2002, vol. 51, pp. 555–565. <http://zhurnal.ape.relarn.ru/articles/2002/051.pdf>.
9. Fleet, M.E., *Acta Cryst.*, 1981, vol. B37, pp. 917–920.
10. Fleet, M.E., *J. Can. Cer. Soc.*, 1982, vol. 51, pp. 13–15.
11. James, R.W., *The Crystalline State*, 1948, London: Bell & Hyman, vol II. Translated under the title *Opticheskie printsipy diffraksii rentgenovskikh luchej*, Moscow: Inostrannaya Literatura, 1950.